Original article

Untargeted and targeted mass spectrometry reveal the effects of theanine on the central and peripheral metabolomics of chronic unpredictable mild stress-induced depression in juvenile rats

Yanru Zhu [a, b], Feng Wang [b], Jiatong Han [b], Yunli Zhao [b], Miao Yu [b], Mingyan Ma [a, *], Zhiguo Yu [b, **]

[a] Laboratory of Pharmaceutical Analysis, School of Pharmacy, Zhejiang Pharmaceutical University, Ningbo, Zhejiang, 315100, China
[b] Laboratory of Pharmaceutical Analysis, School of Pharmacy, Shenyang Pharmaceutical University, Shenyang, 110016, China

ARTICLE INFO

ABSTRACT

L-theanine has been shown to have a therapeutic effect on depression. However, whether L-theanine has an excellent preventive effect on depression in children and adolescents and what its mechanism is have not been well explained. Given the complexity of the pathogenesis of depression, this study investigated the preventive effect and mechanism of L-theanine on depression in juvenile rats by combining serum and hippocampal metabolomic strategies. Behavioral tests, hippocampal tissue sections, and serum and hippocampal biochemical indexes were studied, and the results confirmed the preventive effect of L-theanine. Untargeted reversed-phase liquid chromatography-quadrupole-time-of-flight mass spectrometry and targeted hydrophilic interaction liquid chromatography-triple quadrupole mass spectrometry were developed to analyze the metabolism changes in the serum and hippocampus to screen for potential biomarkers related to L-theanine treatment. The results suggested that 28 abnormal metabolites in the serum and hippocampus that were considered as potential biomarkers returned to near-normal levels after L-theanine administration. These biomarkers were involved in various metabolic pathways, mainly including amino acid metabolism and lipid metabolism. The levels of amino acids and neurotransmitters in the phenylalanine, tryptophan, and glutamic acid pathways were significantly reduced after L-theanine administration compared with chronic unpredictable mild stress-induced rats. In summary, L-theanine had a significant preventive effect on depression and achieved its preventive results on depression by regulating various aspects of the body, such as amino acids, lipids, and inflammation. This research systematically analyzed the mechanism of L-theanine in preventing depression and laid the foundation for applying L-theanine to prevent depression in children and adolescents.

© 2022 The Author(s). Published by Elsevier B.V. on behalf of Xi'an Jiaotong University. This is an open access article under the CC BY-NC-ND license (http://creativecommons.org/licenses/by-nc-nd/4.0/).

1. Introduction

Depression and anxiety, which usually first appear during adolescence, are the most common mental health problems [1]. A representative epidemiological study showed that the lifetime prevalence of depression in adolescents aged 15–18 years is between 11% and 14%, and approximately 20% of adolescents aged 18 years suffer from major depression [2]. Anxiety and depression have become the most significant health issues for the adolescent healthcare sector [3], constituting a significant public health burden. The complex mechanisms of depression include the monoamine hypothesis, receptor hypothesis, neuroinflammation hypothesis, and neuroendocrine hypothesis [4]. A large number of studies have been carried out recently to clarify the pathogenesis of depression. The monoamine hypothesis states that the biological essence of depression is insufficient levels of the monoamine neurotransmitters serotonin (5-HT), norepinephrine (NE), and dopamine (DA). With the development of immunological research, studies showed that the immune function of patients with

depression changed, mainly in the level of cytokines [5], which is the main content of the neuroendocrine hypothesis. The abnormal glutamatergic neurotransmission associated with the *N*-methyl-D-aspartic acid (NMDA) receptor is also considered to be integral to the pathophysiology of depression [6]. Due to differences in drug metabolic enzymes, adolescents may have up to 30% lower exposure to escitalopram and sertraline and three times higher exposure to fluoxetine and fluvoxamine compared with adults [3]. Whilst adolescents and adults respond differently to antidepressants, the current treatment of depression for adolescents is mainly based on that for adults. In a previous study on acute depression in children and adolescents, amongst the 14 antidepressants, only fluoxetine was significantly more effective than the placebo. Imipramine, venlafaxine, and duloxetine were discontinued due to adverse reactions [7]. Therefore, it is vital to develop new antidepressants and implement effective treatment plans for adolescents.

L-theanine is a biologically active ingredient in green tea, a food additive closely related to health. The neuroprotective effects of L-theanine on mental illnesses, such as anxiety, panic, depression and obsessive-compulsive disorder, have been observed [8]. A randomized, double-blind and placebo-controlled trial showed that adults taking L-theanine for four weeks had reduced stress and improved cognitive function and sleep quality [9]. Recently, the antidepressant effect of L-theanine has received extensive attention from researchers [10,11]. In particular, L-theanine is very safe and can be used up to a dose of 4000 mg/kg/day [12] and the acute, subacute, chronic, genetic toxicity, and mutagenicity research results also showed that it is safe [13]. However, the effects of L-theanine on depression in adolescents and its mechanism of action need further research.

Metabolomics is a branch of omics and focuses on the high-throughput identification and quantification of small-molecule (<1500 Da) metabolites. It is widely used due to its high sensitivity, resolution, and throughput [14]. Untargeted metabolomics provides a global view of endogenous metabolic fluctuations in response to exogenous stimuli, which has been widely used to explore the changes of endogenous metabolites stimulated by exogenous substances [15], define the pathogenesis of diseases [16], and identify metabolite biomarkers for diagnosis and prognosis. Targeted metabolomics analysis based on triple quadrupole mass spectrometer coupled with multiple reaction monitoring (MRM) mode has been the gold standard for metabolite quantification [6] and is widely applied in metabolomics verification.

In this study, we replicated the chronic unpredictable mild stress (CUMS) rat model of depression recognized by the international psychopharmacology community and investigated the hypothesis of the pathogenesis of depression. First, reversed-phase ultra-high-performance liquid chromatography-quadrupole-time-of-flight mass spectrometry (RP-UPLC-Q-TOF-MS/MS) was used to perform untargeted metabolomics analysis of metabolism changes in the serum and hippocampus to screen potential biomarkers related to L-theanine's preventive effects on depression in CUMS-induced depressed rats. Then, a hydrophilic interaction liquid chromatography-triple quadrupole mass spectrometry (HILIC-QQQ-MS/MS) analysis was developed to determine the amino acids and neurotransmitters in the pathway of phenylalanine (Phe), tryptophan (Trp), and glutamic acid (Glu) metabolism (Fig. 1) in the rat serum and hippocampus. The levels of inflammatory factors were measured by enzyme-linked immunosorbent assay (ELISA). Finally, the antidepressive effect of L-theanine and its related mechanisms were evaluated in juvenile rats and compared with those of fluoxetine. This study provides a foundation for the clinical application of L-theanine in treating adolescent depression.

2. Materials and methods

2.1. Materials and reagents

5-HT (98.0% purity by high performance liquid chromatography (HPLC)) was obtained from Sigma (St. Louis, Missouri, USA). DA (98.0% purity by HPLC) was obtained from Shanghai Maclin Biochemical Technology Co., Ltd. (Shanghai, China). NE (98.0% purity by HPLC), L-Gln (98.0% purity by HPLC), L-Glu (98.0% purity by HPLC), 3,4-dihydroxyphenylacetic acid (DOPAC, 98.0% purity by HPLC), and 5-hydroxytryptophan (5-HTP, 98.0% purity by HPLC) were obtained from Shanghai Xiyuan Biotechnology Co., Ltd. (Shanghai, China). 3-methoxy-4-hydroxyphenylglycol (MHPG, 98.0% purity by HPLC) was obtained from Toronto Research Chemicals (Toronto, Canada). L-tyrosine (L-Tyr, 99.0% purity by HPLC), L-Phe (98.0% purity by HPLC), and L-Trp (98.0% purity by HPLC) were obtained from Shanghai Yuanye Biological Technology Co., Ltd. (Shanghai, China). [^{2}H$_5$]-L-Glu (99.0% purity by HPLC) was obtained from Shanghai Zhenzhun Biological Technology Co., Ltd. (Shanghai, China). L-theanine (99.31% purity, food grade) was obtained from Shandong Qilu Biological Technology Co., Ltd. (Jinan, China). Fluoxetine was produced by Lilly Pharmaceutical Co., Ltd. (Suzhou, China). Acetonitrile and methanol (HPLC grade) were bought from Sigma. Formic acid and ammonium acetate (HPLC grade) were purchased from Concord Technology Co., Ltd. (Tianjin, China). Normal saline was produced by Jilin Kelun Cornell Pharmaceutical Co., Ltd. (Jilin, China). Distilled water was supplied by the Milli-Q Integral 10 system (Merck Millipore, St. Louis, MO, USA). All other reagents were of analytical grade.

2.2. Animals

Specific pathogen-free healthy male Sprague-Dawley rats (SD, four weeks old, licenses No.: SCXK, 2020-0001) were purchased from the Experimental Animal Center of Shenyang Pharmaceutical University (Shenyang, China). All studies were carried out under the principles for animal experimentation of Shenyang Pharmaceutical University. The protocol was approved by the Animal Ethics Committee of Shenyang Pharmaceutical University (No. 211002300068117).

2.3. Molecular docking

Drug treatment for depression primarily targets the monoaminergic nervous system. However, new antidepressants such as the NMDA receptor, one of the ionotropic Glu receptor subtypes, target other brain systems. NMDA receptor contains two Glu and two glycines' recognition sites [17]. The structure of a protein encoded as the 5H8S was downloaded from the Protein Data Bank (http://www.rcsb.org/), and the structure of the NMDA receptor was isolated from the 5H8S using PyMOL 2.0; the five primary amino acid residues, namely, Arg96, Thr91, Glu193, Tyr61, and Ser142, in the NMDA receptor were selected for cavity positioning. The structure of L-theanine was drawn with Chemdraw 19.0. AutoDock 1.5.6 was used to dock the NMDA receptor and L-theanine semi-flexible and finally processed using PyMOL 2.0.

2.4. Drugs and groups

L-theanine and fluoxetine dissolved in purified water were ultrasonically mixed and administered in a constant dose of 10 and 2 mg/kg/day, respectively. During adaptive feeding for 7 days, the base value of the open field test (OFT), sucrose preference test (SPT), body weight (BW), and food intake (FI) were measured. The rats
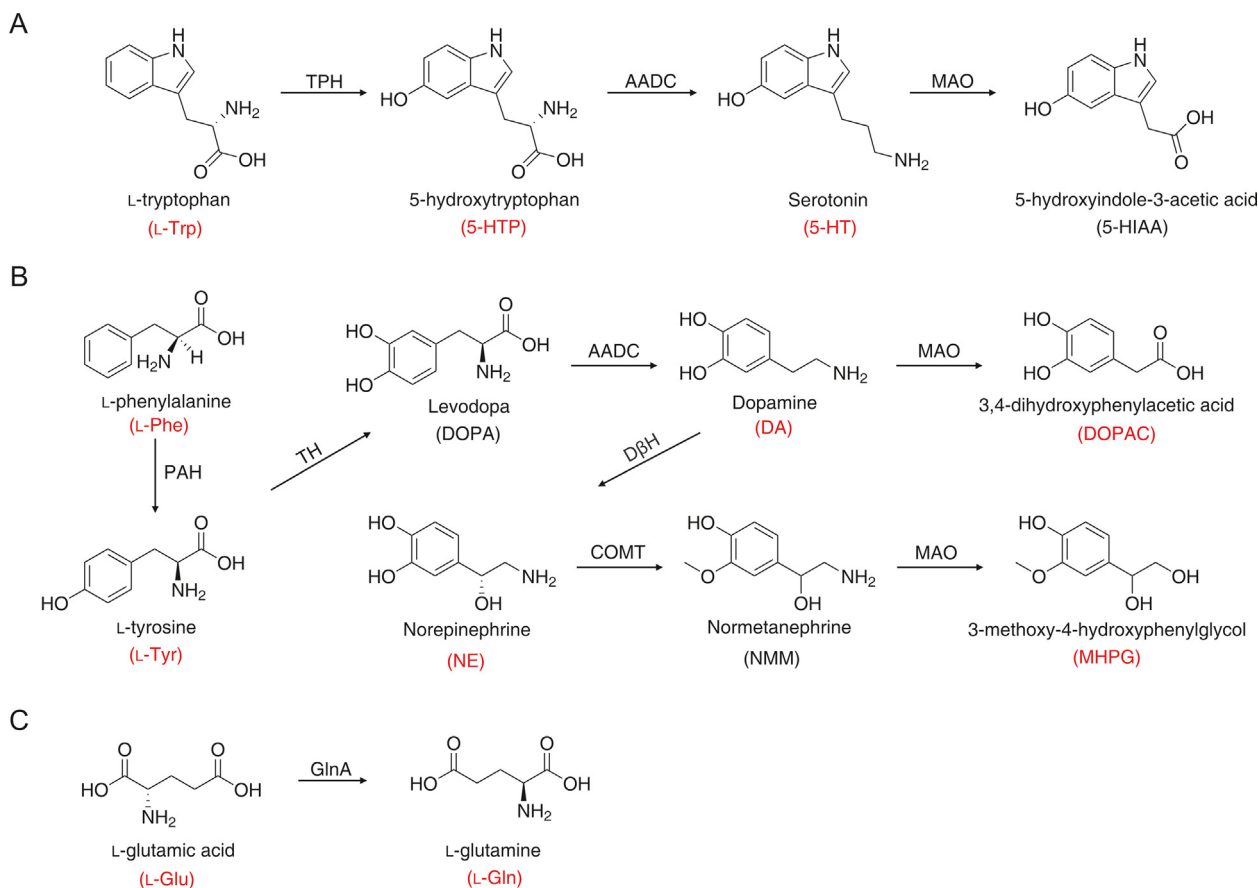
Fig. 1. Structures and metabolic transformation of the compounds used in the study. (A) Tryptophan (Trp) metabolic pathway, (B) phenylalanine (Phe) metabolic pathway, and (C) glutamic acid (Glu) metabolic pathway. TPH: Trp hydroxylase; AADC: aromatic ʟ-amino acid decarboxylase; MAO: monoamine oxidase; PAH: Phe hydroxylase; TH: tyrosine hydroxylase; DβH: dopamine beta hydroxylase; COMT: catechol-*O*-methyltransferase; GlnA: glutamine synthetase.

were divided into the normal control group (N-Con, $n = 6$), normal administration group (N-Thea, $n = 6$), model control group (M-Con, $n = 6$), model administration group (M-Thea, $n = 6$), and positive administration group (M-Flu, $n = 6$) according to the score. The grouping and dosage are shown in Table 1. Intragastric administration started at 8 a.m. every day.

2.5. CUMS model procedure

N-Con and N-Thea were raised in combined cages, whereas the others were raised in solitary cages and subjected to CUMS to establish depression models [18]. SD rats in M-Con, M-Thea, and M-Flu received continuous stimulation for 4 weeks, with one or two random stimuli after 1 h of administration every day. Stimulus

factors involved tail clamping (2 min), heat stress (45 °C, 10 min), co-cage rearing (6 h), empty bottle placement (6 h), tilting the squirrel cage (12 h), wet litter (12 h), placement of unknown objects (12 h), flash lighting (12 h), day and night upside-down (24 h), water prohibition (24 h), and fasting (24 h). Additionally, the same stimulus did not reappear within two days.

2.6. Behavioral testing

The SPT, BW, and FI were measured on Monday, Wednesday, and Thursday each week, respectively. The OFT, forced swimming test (FST), and light/dark box test (LDB) were implemented after the model was established.

2.6.1. SPT

During the adaptation period, two bottles were placed in each cage. The two bottles contained 1% (m/V) sucrose solution in the first 24 h, and the solution in one bottle was changed to purified water for the following 24 h for adaptability training. The SPT was performed after 24 h of food and water deprivation. The presence of 150 mL of 1% (m/V) sucrose solution and 150 mL of purified water were given. The test time was fixed for 6 h, and the position of the bottles was interchanged to ensure that rats did not develop a side preference. The sucrose consumption and purified water consumption were measured to calculate the sucrose preference index.

Table 1
Grouping and dosing regimen for pharmacodynamic experiments ($n = 6$).

Group	Drug	Concentration (mg/mL)	Administration	Dose (mg/kg)
N-Con	Water	3.0	i.g.	10
N-Thea	ʟ-theanine	3.0	i.g.	10
M-Con	Water	3.0	i.g.	10
M-Thea	ʟ-theanine	3.0	i.g.	10
M-Flu	Fluoxetine hydrochloride	0.6	i.g.	2

N-Con: normal control group; N-Thea: normal administration group; M-Con: model control group; M-Thea: model administration group; M-Flu: positive administration group; i.g.: intragastric administration.

2.6.2. OFT

The chamber (60 cm × 40 cm × 60 cm) with opaque sidewalls and black bottom divided into 24 cells with white lines was used for the OFT. The rats were put in the middle grid with the heads facing the same direction. The rats' scores of standing upright, grooming, or crossing the grid were recorded. The chamber was cleaned with alcohol to remove the odor of other rats after each measurement.

2.6.3. FST

Pre-swim training was implemented to the rats for 10 min. The rats were placed in a test bucket with an inner diameter of 30 cm and a height of 60 cm filled with water. The immobility time of the rats was recorded and quietness was maintained during testing.

2.6.4. LDB

Two identical boxes (40 cm × 40 cm × 60 cm), a blackout box, and a bright box with lighting, were connected by a 60-cm sealed channel. The rats were placed in the dark box, and the number of times the rats crossed into the bright box and the stay time were recorded. Going across to the bright box each time or staying in the bright box each second would be counted as one point.

2.7. Tissue sections

The rats were sacrificed by decapitation, and the brains were immediately separated. Then, half the brain was fixed in 4% para-formaldehyde and embedded in wax blocks. After sectioning, hematoxylin-eosin (H&E) staining, and mounting, the hippocampal pathology was observed under an optical microscope.

2.8. Assay of biochemical indicators

After 28 days of modelling, 0.3 mL of blood was collected and centrifuged at 1,110 g for 10 min after standing for 1 h at room temperature. The supernatant was collected to prepare serum samples. The weight of the hippocampus was measured and recorded, and the precooled saline was added at a ratio of 1:9 (m/V). The hippocampus homogenate was prepared under the ice bath condition by an ultrasonic cell crusher (Scientz, Ningbo, China). Interleukin (IL)-1β, IL-10, and tumor necrosis factor alpha (TNF-α) were obtained from Jiangsu Baolai Biotechnology (Nanjing, China), and determination was performed by ELISA kits according to the manufacturer's protocol.

2.9. Instrumentation and conditions

2.9.1. Untargeted metabolomics

Samples were analyzed by high-resolution Xevo G2 XS Q-Tof-MS/MS with ACQUITY UPLCI-Class UPLC system (Waters, Milford, MA, USA), equipped with an electrospray ionization (ESI) source. An ACQUITY UPLC HSS T$_3$ column (2.1 mm × 100 mm, 1.8 μm; Waters, Milford, MA, USA) was used to complete chromatographic separation at 35 °C. Elution was accomplished using the mobile phase of 0.1% formic acid:water (V/V) (A) and acetonitrile (B) at a flow rate of 0.4 mL/min. The analytes were eluted using the following gradient elution method: 0−1 min, 98% A; 1−7 min, 98%−50% A; 7−17 min, 50%−25% A; 17−20 min, 25%−5% A; 20−23 min, 5% A; 23−23.1 min, 5%−98% A; and 23.1−25 min, 98% A.

Full scan was acquired over a mass range of m/z 50−1500 in both positive-ion mode and negative-ion mode. The parameters were as follows: collision energy, low/off and high/15−45 eV; capillary voltage, 2.5 kV; cone voltage, 30 V; ion source temperature, 120 °C; atomizing gas temperature, 500 °C; cone gas flow rate, 50 L/h; and atomization gas flow rate, 800 L/h. The retention time and peak areas of the standard quality control (QC) samples were used to assess the data quality. The chromatograms and data were acquired by MassLynx V4.1 and Progenesis QI software.

2.9.2. Targeted metabolomics

The samples were analyzed by SCIEX Triple Quad™ 4500 liquid chromatography-tandem mass spectrometry (LC-MS/MS) system (SCIEX, Framingham, MA, USA) with Agilent 1260 HPLC system (Agilent, Palo Alto, CA, USA), equipped with an ESI source. Chromatographic separation was completed on an Agilent ZORBAX RR HILIC Plus 95Å column (100 mm × 2.1 mm, 3.5 μm) at 35 °C. The elution was accomplished using water containing 0.2% (V/V) formic acid and 0.005 mol/L ammonium acetate (A) and acetonitrile containing 0.2% (V/V) formic acid (B). The analytes were eluted using a gradient elution method as follows: 0−0.5 min, 35% A; 0.5−2 min, 35%−50% A; 2−2.5 min, 50% A; 2.5−2.6 min, 50% A−35% A; and 2.6−4.5 min 35% A, at a flow rate of 0.3 mL/min.

The mass spectrometer was operated in the positive ion mode using MRM. Collision energy, declustering potential, and ion fragments are shown in Table 2 and Fig. S1. The other parameters were as follows: ion spray voltage of 4500 V, source temperature of 500 °C, collision gas at 12 psi, ion source gas I at 40 psi, gas II at 40 psi, and curtain gas at 20 psi. The chromatograms and data were acquired by Analyst 1.6.3 software (SCIEX).

2.10. Method validation

2.10.1. Untargeted metabolomics

The hippocampus and serum samples of each group were taken and mixed in equal volumes to prepare QC samples for method verification. Principal component analysis (PCA) was performed on all samples after data preprocessing, and the aggregation degree of QC samples was observed in the score plot. System repeatability, method repeatability, sample stability, and system stability were obtained by calculating the relative standard deviation (RSD) or relative error (RE) of the retention time (t_R) and the peak area.

2.10.2. Targeted metabolomics

The HILIC-QQQ-MS/MS method was validated according to the Bioanalytical Method Validation, Guidance for Industry of the U.S. Food and Drug Administration [19]. Linearity, accuracy, precision, carryover, dilution evaluation, recovery, matrix effect, and stability were assessed. The low limits of quantitation (LLOQs) of the analytes were 0.1, 0.1, 0.1, 0.01, 0.05, 0.01, 0.05, 0.05, 0.01, 0.1, and 0.1 μg/mL for L-Phe, L-Trp, L-Tyr, DA, NE, 5-HT, DOPAC, MHPG, 5-HTP, L-Glu,

Table 2
Optimized multiple reaction monitoring (MRM) parameters, declustering potential (DP), and collision energy (CE) for neurotransmitters and internal standard (IS).

Analyte	Precursor ion (m/z)	Product ion (m/z)	DP (V)	CE (eV)
L-Phe	166.0	120.1	10	17
L-Tyr	181.9	164.9	10	13
L-Trp	205.0	149.0	12	7
DA	154.1	136.9	11	12
NE	170.0	152.1	6	10
5-HT	177.0	160.0	7	13
DOPAC	169.1	134.8	5	9
MHPG	263.0	201.4	49	25
5-HTP	221.0	204.1	16	14
L-Glu	148.0	84.0	10	19
L-Gln	147.1	84.1	12	24
IS	153.0	88.2	12	21

L-Phe: L-phenylalanine; L-Tyr: L-tyrosine; L-Trp: L-tryptophan; DA: dopamine; NE: norepinephrine; 5-HT: serotonin; DOPAC: 3,4-dihydroxyphenylacetic acid; MHPG: 3-methoxy-4-hydroxyphenylglycol; 5-HTP: 5-hydroxytryptophan; L-Glu: L-gluta-mic acid; L-Gln: L-glutamine.

and L-Gln, respectively, while the upper limits of quantification were 10, 10, 10, 1, 5, 1, 5, 5, 1, 10, and 10 μg/mL, respectively. All validation experiments were performed in alternative matrix methanol:water (1:1, *V/V*) because of the variable endogenous level in depression [20], except for matrix effect and recovery, which were performed in the serum and hippocampus, to compare the extraction and ionization efficiencies between biological matrices. The level of spiked analytes was 20 times the average concentration of biological samples in healthy rats, which made the analyte concentration in the body less than 5% of the measured value. The actual matrix samples were analyzed together with the simulated QC samples to evaluate the stability. Preparation of calibration standards and QCs and the method validation process were shown in the Supplementary data.

2.11. Preparation of biological samples

For the untargeted metabolomics study, 300 μL of cold aceto-nitrile was used for protein precipitation to eliminate protein interference in 100 μL of serum. For targeted metabolomics study, 100 μL of serum was mixed with 10 μL of IS and 10 μL of methanol, and protein was precipitated with 300 μL of 0.1% formic acidified acetonitrile. All serum samples were vortexed for 5 min after adding precipitation protein solvent and centrifuged at 10,010 *g* for 15 min at 4 °C. The supernatant was dried under nitrogen flow. Before being injected into the LC-MS system, the residue was reconstituted in 100 μL of initial mobile phase, vortexed, and centrifuged to remove the insoluble material. For the untargeted metabolomics study, the homogenization operation of the hippo-campus was the same as the assay of biochemical indicators with methanol:water (4:1, *V/V*) as homogenization solvent, whereas the operation was the same as the assay of biochemical indicators for targeted metabolomics study. The processes of hippocampal sam-ples were similar to those of serum samples.

2.12. Data processing and statistical analyses

RP-UPLC-Q-TOF-MS/MS data (.RAW) were imported into Pro-genesis QI for peak alignment, detection, and deconvolution for untargeted metabolomic analysis. The sample data with the mini-mum coefficient of variation > 30% were excluded, and PCA and partial least square discriminant analysis (PLS-DA) was performed to screen potential differential compounds. The adjusted *P* value was calculated through a log-normalized one-way analysis of variance test. Substances with statistically significant differences

($P < 0.05$) were selected. The fold change in the intensity of features was calculated with the threshold of greater than or equal to 2, and the variable importance in the projection value of metabolites was greater than 1 to look for potential biomarkers with retention time within 20 min. The threshold precursor tolerance (10 ppm) and fragment tolerance (10 ppm) were set to carry out structural identification in Human Metabolome Database (http://www.hmdb. ca/), METLIN MS/MS (http://metlin.scripps.edu/), Kyoto Encyclo-pedia of Genes and Genomes (http://www.genome.jp/kegg/ligand. html), LipidMaps (https://lipidmaps.org/), and LipidBlast (https:// fiehnlab.ucdavis.edu/) databases. The visual metabolism analysis of pathways was completed using MetaboAnalyst (version 5.0, https://www.metaboanalyst.ca/). The data were presented as mean ± standard deviation. Statistical analysis was performed us-ing IBM SPSS Statistics 25 (SPSS Inc., Chicago, IL, USA). *P < 0.05 indicated significant differences, **P < 0.01 indicated very signifi-cant differences, and ns indicated no significant differences. The figures were created by Origin 2021 (Northampton, MA, USA) and GraphPad Prism 5.01 (San Diego, CA, USA).

3. Results and discussion

3.1. Molecular docking

AutoDock 1.5.6 was used to simulate the specific recognition of L-theanine and the NMDA receptor. The H and O of Arg96, Thr91, Glu193, and Ser142 residues in the NMDA receptor and the O and H of L-theanine interacted via hydrogen bonds. The benzene ring conjugate system of Tyr61 and the N atomic system of L-theanine interacted via van der Waals as shown in Fig. 2. The binding energy was −8.44 kcal/mol and the unbound extended energy was −1.78 kcal/mol. As the binding energy was <0, L-theanine could spontaneously combine with the NMDA receptor and exert therapeutic effects through Glu receptors. Converging evidence indicated that the glutamatergic system was directly implicated in the pathophysiology of depression [21]. Yu et al. [22] suggested that CUMS might induce depression through overactivation of NMDA receptors, and the molecular docking result suggested that L-the-anine might exert antidepressant effects by inhibiting NMDA re-ceptor overactivation.

3.2. Behavioral tests

Growing evidence suggested that chronic stress plays a sig-nificant role in the pathophysiology of depression, and the CUMS
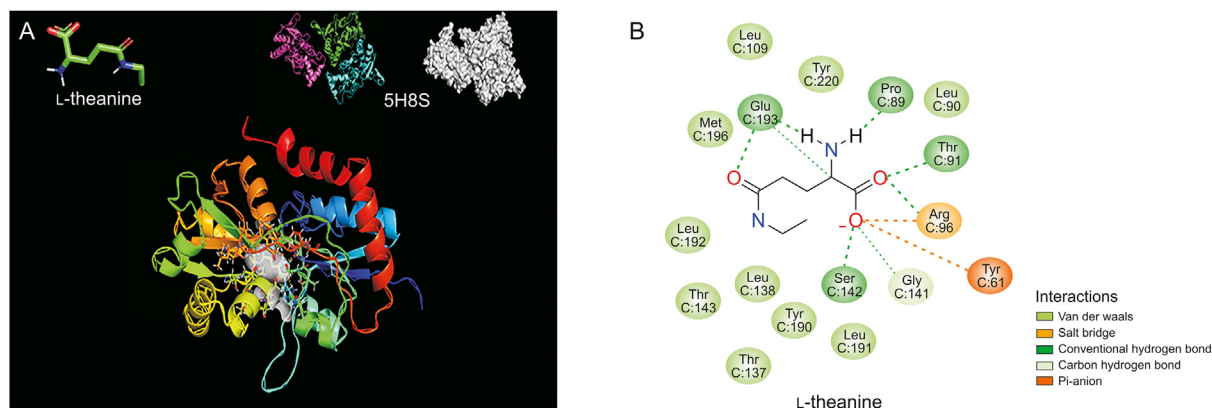

Fig. 2. Targeting ability and characterization of the L-theanine. (A) The specific recognition of L-theanine and the *N*-methyl-D-aspartic acid (NMDA) receptor isolated from the 5H8S. (B) The two-dimensional image of the docking result of L-theanine and NMDA receptor isolated from the 5H8S.
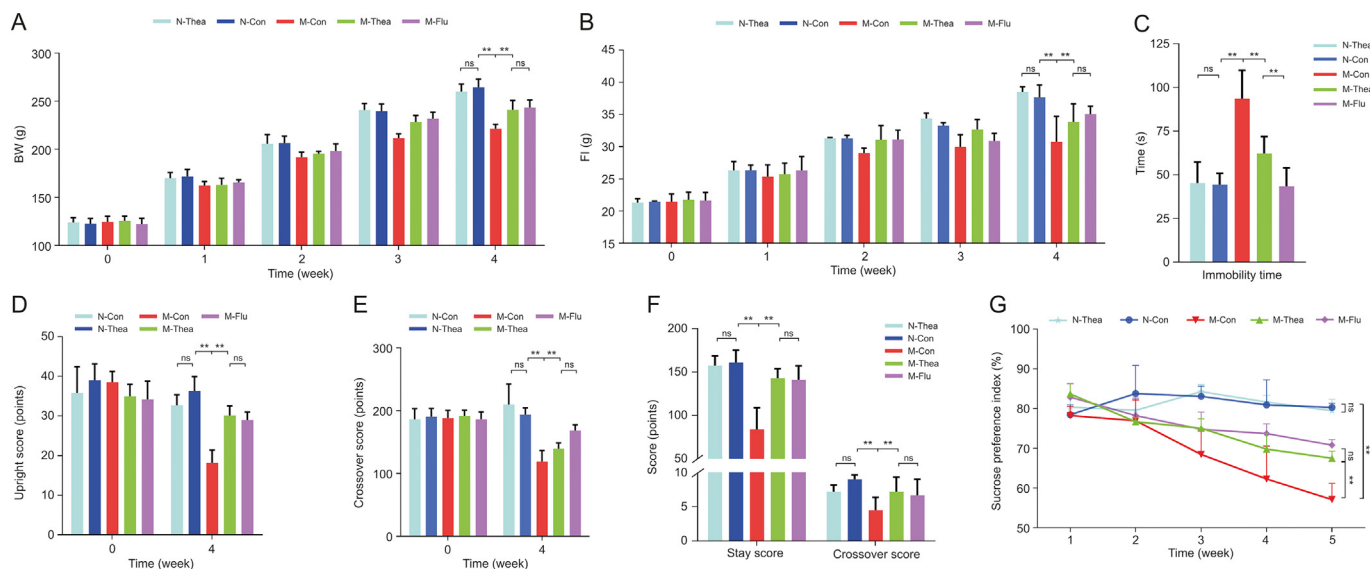
Fig. 3. Behavioral differences of rats among various groups. (A) Body weight (BW); (B) food intake (FI); (C) forced swimming test (FST); (D) upright score in open field test (OFT); (E) crossover score in OFT; (F) light/dark box test (LDB); and (G) sucrose preference test (SPT). Values were calculated as mean ± standard deviation ($n = 6$). $^{**}P < 0.01$, very significant differences; ns: no significant differences. N-Thea: normal administration group; N-Con: normal control group; M-Con: model control group; M-Thea: model administration group; M-Flu: positive administration group.

model was established through chronic randomization of different low-intensity stress factors to induce depressive status in rats [23], which was similar to the clinical symptoms of depressive patients, and widely used in screening anti-depressant drugs [24]. Behavioral tests are important and widely performed to evaluate whether drugs possess antidepressant activity [23]. SPT is a reward-based behavioral detection method, and reduced responsiveness to rewards is one of the core characteristics of depression. OFT is based on exploration, and studies showed that the greater the depression of rats, the less their activity in the field [25]. FST is a desperate behavioral test method that has good predictive validity and can evaluate the effectiveness of antidepressants through immobility time [26]. LDB is based on the innate aversion to brightly illuminated areas and the spontaneous exploration of new environments and light of rodents [27]. We observed an insignificant variance amongst various groups ($P > 0.05$) before modelling, while very significant differences were presented in M-Con and N-Con after modelling in BW, FI, SPT, and OFT in Fig. 3. Compared with N-Con, the scores of M-Con in LDB dropped significantly, whereas the immobility time in FST was significantly increased ($P < 0.01$), which indicated the successful duplication of the CUMS model. M-Thea significantly reversed the indexes compared with M-Con ($P < 0.01$) and showed almost no significant differences ($P > 0.05$) with M-Flu in BW, FI, LDB, and upright times in OFT, which initially suggested that L-theanine has a specific antidepressant effect on juvenile rats. N-Con showed no significant differences with N-Thea, indicating that L-theanine has no impact on the growth of juvenile rats and could be administered in children.

3.3. H&E staining results of the hippocampus

The hippocampus is an integral part of the limbic system and is generally divided into the hippocampal gyrus and dentate gyrus according to cell morphology. The hippocampal gyrus is mainly composed of pyramidal neurons, including the CA1, CA2, CA3, and CA4 regions [28]. Pyramidal neurons in the CA1 area of the hippocampus are the primary cell type of hippocampal neurons and are closely related to depression [29]. Fig. 4 shows that the

pyramidal cells in the CA1 region of the hippocampus in N-Con and N-Thea were neatly arranged and had regular morphology, full cells, and clear nucleus. The structure was apparently damaged, pyramidal cells were arranged disorderly, some neurons were lost, the cell body was empty, and the space around the cells was enlarged in M-Con. Compared with M-Con, the neuronal cell damage of M-Thea and M-Flu was less severe, the cell morphology was more regular, the arrangement was restored, and the empty staining was reduced. This indicated that L-theanine had no damage to the brain tissue, whereas long-term stress stimulation caused damage to the rat brain, including damaged or missing neurons. Thus, L-theanine had a significant improvement effect.

3.4. Cytokine studies

The inflammation hypothesis has received more attention in the pathogenesis of depression. According to the cytokine hypothesis, depression may be triggered and aggravated by psychosocial and internal stressors through inflammatory processes, and levels of pro-inflammatory cytokines may be one of the important
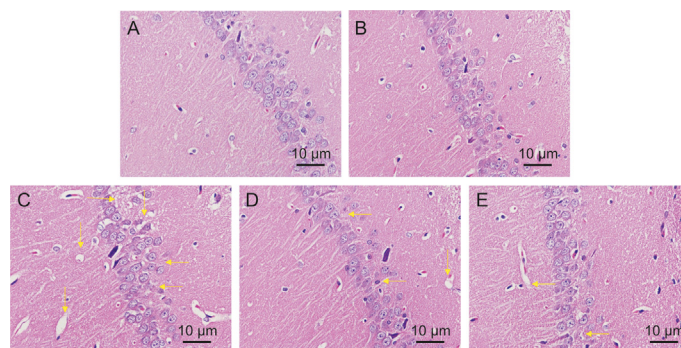

Fig. 4. CA1 region of hippocampus histopathology of various groups (400×). (A) N-Con, (B) N-Thea, (C) M-Con, (D) M-Thea, and (E) M-Flu. N-Con: normal control group; N-Thea: normal administration group; M-Con: model control group; M-Thea: model administration group; M-Flu: positive administration group.

mechanisms leading to depression [30]. Compared with N-Con, the anti-inflammatory cytokine IL-10 was significantly decreased ($P < 0.05$), and the pro-inflammatory cytokines TNF-α and IL-1β were significantly increased ($P < 0.01$) in the serum and hippocampus of M-Con. M-Thea could reverse these changes compared with M-Con and no significant differences were observed compared with M-Flu ($P > 0.05$). There was no significant difference ($P > 0.05$) between N-Con and N-Thea in the serum and hippocampus (Fig. 5). This indicated that CUMS could activate rat brain microglia, release pro-inflammatory cytokines, activate indoleamine-2,3-dioxygenase, and lead to a decrease in serotonin in the corresponding part, thereby causing depression-like symptoms [31]. L-theanine had anti-inflammatory effects and did not affect the health status.

3.5. Method validation

For untargeted metabolomics, system repeatability, method repeatability, sample stability, and system stability were validated with QC samples of serum and hippocampus in the positive and negative modes. The results were acceptable as shown in Table S1 and Fig. S2. At present, the background subtraction method [32,33] is often used to simplify the pre-processing method of

neurotransmitter determination and obtain accurate results. However, this method is only suitable for determination when the level of endogenous substances is consistent. It is difficult to determine the variable endogenous level such as in depression. The alternative matrix method is used to avoid this problem, which requires similar matrix effect and extraction recoveries in the alternative and original matrix [34,35]. The chromatograms of six batches of actual biological samples and alternative matrix samples spiked with standard solutions were obtained to evaluate the specificity, as shown in Fig. S3. Targeted metabolomic analytes exhibited satisfactory linearity within their corresponding range, as shown in Table S2. As shown in Table S3, the accuracy (RE) of the LLOQs was within ±20% and the accuracy (RSD) was within 20%. The concentration of QC samples was used to evaluate the precision and accuracy. The results were acceptable as shown in Table 3 (Table S3). The absolute values of RE and RSD were less than 15%. The extraction recovery and matrix effect of each analyte were acceptable as shown in Table 3 (Table S4). However, DOPAC in the serum and hippocampus, DA in the serum, and 5-HTP in the hippocampus with a strong matrix effect did not meet the analytical requirements. The impact of carryover on the blank samples following the highest calibration sample was assessed and carry-over was less than 20% of the LLOQ and less
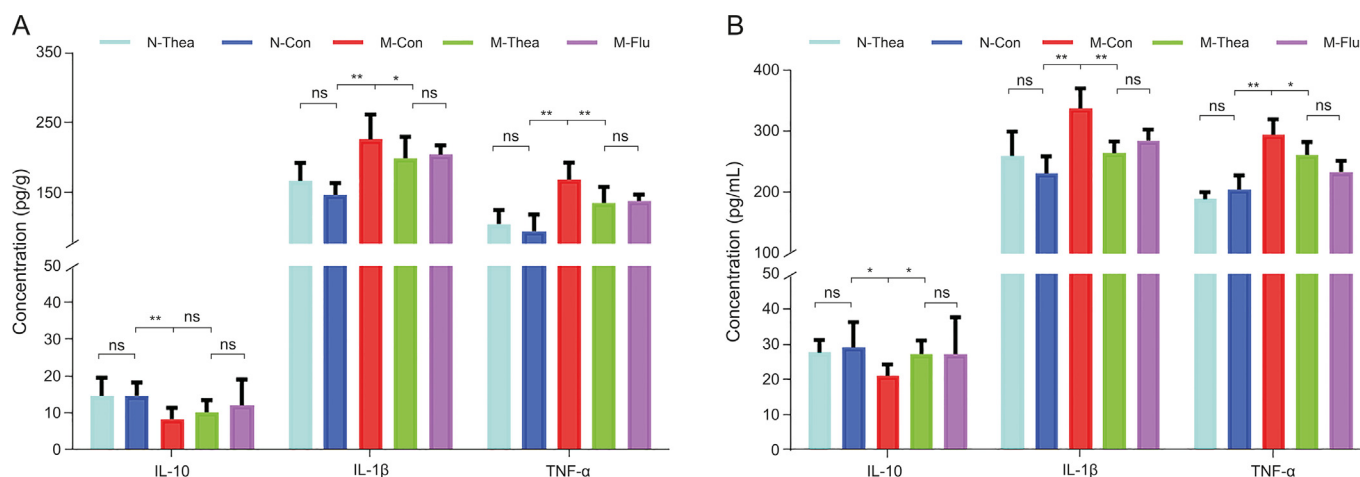

Fig. 5. Levels of related cytokines in (A) hippocampus and (B) serum among various groups. Values were calculated as mean ± standard deviation ($n = 6$). ** $P < 0.01$, very significant differences; * $P < 0.05$, significant differences; ns: no significant differences. N-Thea: normal administration group; N-Con: normal control group; M-Con: model control group; M-Thea: model administration group; M-Flu: positive administration group; IL: interleukin; TNF-α: tumor necrosis factor alpha.

Table 3
Validation results for the targeted method at quality control (QC) medium levels ($n = 6$).

Analyte	Precision (RSD)	Accuracy (RE)	Serum (%)		Hippocampus (%)	
			Extraction recovery	Matrix effect	Extraction recovery	Matrix effect
L-Phe	4.2	−1.6	97.3 ± 5.1	103.2 ± 6.0	101.1 ± 11.2	96.3 ± 8.2
L-Tyr	5.4	−1.4	100.8 ± 3.6	101.2 ± 4.3	103.2 ± 7.2	101.3 ± 6.5
L-Trp	3.4	−3.1	87.9 ± 5.5	90.4 ± 8.1	98.6 ± 2.4	101.4 ± 6.2
DA	3.6	2.4	—	—	86.3 ± 9.0	99.4 ± 11.6
NE	3.5	−4.2	95.1 ± 6.3	94.8 ± 7.7	99.2 ± 9.6	96.4 ± 5.4
5-HT	5.0	−1.4	100.0 ± 2.6	99.2 ± 1.6	97.4 ± 6.1	99.5 ± 3.7
DOPAC	2.2	−0.2	—	—	—	—
MHPG	4.0	−2.4	99.6 ± 2.1	99.6 ± 2.6	100.0 ± 2.7	97.3 ± 3.0
5-HTP	3.7	1.3	84.1 ± 3.5	86.9 ± 4.1	—	—
L-Gln	4.9	0.7	99.9 ± 2.7	101.9 ± 1.9	100.3 ± 2.8	98.8 ± 3.1
L-Glu	4.6	2.0	97.9 ± 3.1	103.8 ± 3.7	97.3 ± 6.1	97.2 ± 7.1

—: not detected in the matrix due to strong matrix effect; RSD: relative standard deviation; RE: relative error; L-Phe: L-phenylalanine; L-Tyr: L-tyrosine; L-Trp: L-tryptophan; DA: dopamine; NE: norepinephrine; 5-HT: serotonin; DOPAC: 3,4-dihydroxyphenylacetic acid; MHPG: 3-methoxy-4-hydroxyphenylglycol; 5-HTP: 5-hydroxytryptophan; L-Glu: L-glutamic acid; L-Gln: L-glutamine.

than 5% of IS. The analytes were diluted 10-fold with alternative matrix to make the final concentration within the range of the standard curve. The accuracy and precision were within ±15% after five replicates were analyzed, which suggested that the concentrations of biological samples over the ULOQ could be accurately quantitated. Stability investigation showed that the RSD was less than 11.3%, and the range of RE was between −8.7% and 11.3% after the samples were frozen for 20 days at −80 °C, placed at room temperature for 8 h, subjected to three freeze-thaw cycles, and placed for 24 h in auto-sampler vials at 4 °C, which met the requirements for biological samples. The information is shown in Table 4.

3.6. Untargeted metabolomics

3.6.1. Multivariate statistical analysis

RP-UPLC-Q-TOF-MS/MS was used to collect the metabolite spectrum information of the rat hippocampus and serum in positive and negative ion modes, respectively. Typical base peak ion intensity chromatograms are shown in Fig. S4. There were significant differences in the relative peak intensities of many ions in chromatograms, indicating that the same substance was different in the five groups, and the profiles of five groups showed much more peaks in the negative ion mode than in the positive one. PLS-DA with supervised pattern recognition could maximize between-group differences and facilitate the search for differential metabolites. The score plots of metabolite data in hippocampus and serum samples of N-Con, N-Thea, M-Con, M-Thea, and M-Flu in the positive and negative ion modes after PLS-DA are shown in Fig. 6A. A total of 200 permutation tests were verified, and the results ($R^2 < 0.4$, $Q^2 < 0$) in Fig. 6B indicated no over-fitting in the model [36]. The position of the samples in the score plot was determined by its endogenous metabolic response. For the same physiological or pathological state, the representative sample points were also similar in the score plot, indicating a close distribution. Therefore, the farther from the blank group, the more severe the deviation of the endogenous metabolic response from the normal physiological state. As shown in the score plot, N-Con and M-Con were separated entirely in the direction of the first principal component (t[1]), whereas M-Thea and M-Flu were between N-Con and M-Con along the direction of t[1]. In summary, the CUMS model was successfully replicated, and L-theanine and fluoxetine hydrochloride had obvious preventive effects on depression in rats. The similar distribution of N-Con and N-Thea along the direction of t[1] reflected that L-theanine had no noticeable impact on healthy rats, which means that it can be used for the prevention of depression in children and adolescents.

3.6.2. Biomarker analysis

A total of 28 potential biomarkers were identified in the hippocampus (Nos. 1−15) and serum (Nos. 16−28) by searching the database (Table 5 and Figs. S5 and S6). Tyr was identified in the hippocampus and serum. Compared with N-Con, M-Con showed alterations in the following metabolites: Glu, xanthine, phosphatidylcholine (PC) (24:1 (15Z)/24:1 (15Z)), enkephalin L, PC (15:0/18:1 (11Z)), phosphatidylethanolamine (PE) (18:1 (11Z)/22:4 (7Z,10Z, 13Z,16Z)), PC (20:1 (11Z)/24:1 (15Z)), corticosterone, lysophosphatidylcholine (LysoPC) (P-18:1 (9Z)), LysoPC (22:1 (13Z)), phenylacetylglycine, PE (18:3 (6Z,9Z,12Z)/22:6 (4Z,7Z,10Z,13Z,16Z,19Z)), and phosphatidylinositol (PI) (18:0/20:4 (5Z,8Z,11Z,14Z)) were upregulated, while Tyr, hypoxanthine, sphingosine, sphingomyelin (SM) (d18:0/18:1 (9Z)), Trp, glycosphingolipids (GlcCer) (d18:1/24:1 (15Z)), threonic acid, 5β-cyprinol sulfate, phosphatidylserine (PS) (18:0/22:6 (4Z,7Z,10Z,13Z,16Z,19Z)), uridine, creatine, cytidine, glycerophosphocholine, and 5-methyltetrahydrofolic acid were down-

Table 4
The stability of analytes in the serum and hippocampus under different conditions (n = 3).

| Analyte | Serum | | | | | | | | | Hippocampus | | | | | | | | |
| | Added concentration (ng/mL) | Short-term stability (8 h) | | Long-term stability (−80 °C for 20 days) | | Three freeze-thaw cycles stability | | Post-preparative samples (24 h at 4 °C) | | Added concentration (ng/mL) | Short-term stability (8 h) | | Long-term stability (−80 °C for 20 days) | | Three freeze-thaw cycles stability | | Post-preparative samples (24 h at 4 °C) | |
		RE (%)	RSD (%)	RE (%)	RSD (%)	RE (%)	RSD (%)	RE (%)	RSD (%)		RE (%)	RSD (%)	RE (%)	RSD (%)	RE (%)	RSD (%)	RE (%)	RSD (%)
L-Phe	300	4.4	4.9	7.6	3.5	−6.3	8.2	6.1	4.1	300	3.9	7.4	−3.6	4.7	5.0	8.5	−3.6	5.2
L-Tyr	300	7.3	5.4	−8.7	5.2	8.5	4.4	3.6	4.2	300	9.4	5.3	7.6	7.3	6.8	5.6	−4.1	7.2
L-Trp	300	7.3	11.3	5.5	7.6	−6.2	9.2	3.1	3.5	300	−3.6	8.3	8.5	4.9	6.9	4.3	5.4	6.2
DA	–	–	–	–	–	–	–	–	–	30	5.7	4.6	4.6	8.7	5.8	4.9	−6.3	5.8
NE	150	3.7	4.6	−5.9	5.7	−6.6	7.7	5.2	−4.1	150	8.3	4.7	6.6	9.8	7.6	9.7	5.1	6.2
5-HT	30	5.4	2.6	9.3	9.6	4.6	4.7	4.2	2.3	30	10.4	8.0	−6.0	7.7	4.7	7.6	−4.3	5.4
MHPG	150	8.2	7.5	6.5	7.0	3.3	7.4	5.2	4.2	150	7.3	4.6	3.0	6.8	7.2	3.6	4.2	5.2
5-HTP	30	−5.7	8.5	10.0	7.5	11.3	7.7	4.2	5.3	–	–	–	–	–	–	–	–	–
L-Gln	300	−6.4	4.6	8.5	7.3	−7.3	6.6	6.2	5.4	300	4.8	6.5	9.6	10.7	3.6	4.7	5.2	6.2
L-Glu	300	4.9	6.3	−4.4	3.9	5.7	7.4	7.1	3.3	300	4.7	7.4	−4.6	9.5	4.6	8.8	6.3	6.4

–: not detected in matrix due to the concentration of endogenous substances in vivo and strong matrix effect; RSD: relative standard deviation; RE: relative error; L-Phe: L-phenylalanine; L-Tyr: L-tyrosine; L-Trp: L-tryptophan; DA: dopamine; NE: norepinephrine; 5-HT: serotonin; 5-HTP: 5-hydroxytryptophan; DOPAC: 3,4-dihydroxyphenylacetic acid; MHPG: 3-methoxy-4-hydroxyphenylglycol; 5-HTP: 5-hydroxytryptophan; L-Glu: L-glutamic acid; L-Gln: L-glutamine.
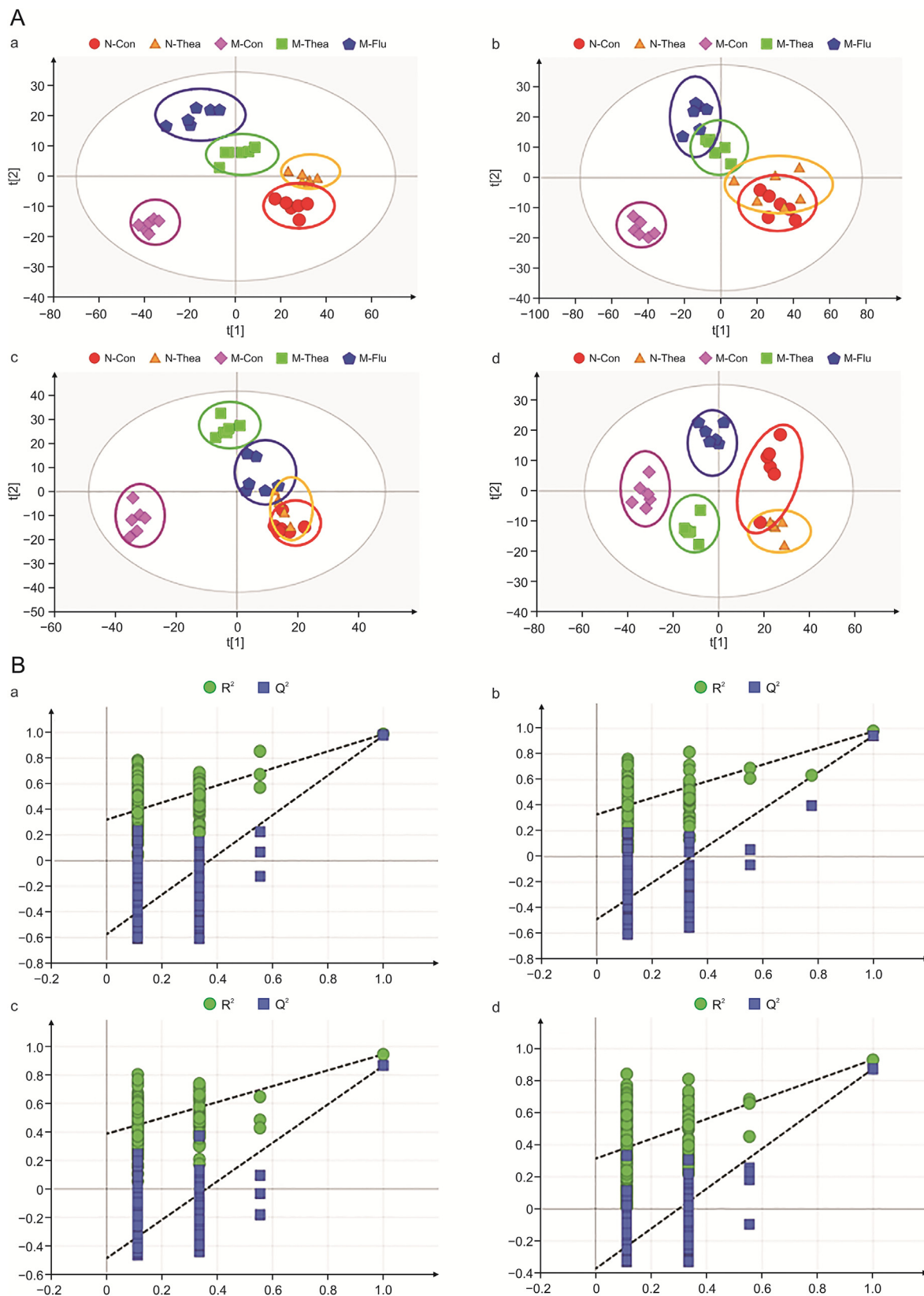
Fig. 6. The results of multivariate statistical analysis. (A) The score plot of partial least square discriminant analysis (PLS-DA) results based on the hippocampus and serum metabolic profiling. The abscissa is the score of the first principal component, the predicted principal component, represented by t[1], and the ordinate is the score of the second principal component, the orthogonal principal component, represented by t[2]. (B) The results of 200 permutation tests. (a) Hippocampus samples in the negative ion mode, (b) hippocampus samples in the positive ion mode, (c) serum samples in the negative ion mode, and (d) serum samples in the positive ion mode. N-Con: normal control group; N-Thea: normal administration group; M-Con: model control group; M-Thea: model administration group; M-Flu: positive administration group.

Table 5
Biomarkers tentatively identified in rat hippocampus and serum.

No.	Compound ID	t_R (min)	Exact mass (Da)	Error (ppm)	Selected ion	Formula	Metabolite identification	Change M-Con	M-Thea	M-Flu	Related pathway
1	HMDB0000148	0.82	147.0532	1.11	$[M+H]^+$	$C_5H_9NO_4$	Glutamic acid	↑##	↓**	↓**	Gln and Glu metabolism
2	HMDB0000292	0.90	152.0334	−0.83	$[M+NH_4]^+$	$C_5H_4N_4O_2$	Xanthine	↑##	↓**	↓**	Purine metabolism
3	HMDB0000158	1.39	181.0739	0.56	$[M+H]^+$	$C_9H_{11}NO_3$	Tyr	↓##	↑**	↑*	Phe, Tyr, and Trp biosynthesis
4	HMDB0000157	2.30	136.0385	−1.71	$[M+H]^+$	$C_5H_4N_4O$	Hypoxanthine	↓##	↑**	↑**	Purine metabolism
5	HMDB0008816	6.93	953.7813	4.48	$[M+H]^+$	$C_{56}H_{108}NO_8P$	PC (24:1 (15Z)/24:1 (15Z))	↑##	−	↓**	Glycerophospholipid metabolism
6	HMDB0000252	15.80	299.2824	1.31	$[M+H]^+$	$C_{18}H_{37}NO_2$	Sphingosine	↓##	↑**	↑**	Sphingolipid metabolism
7	HMDB0012089	19.90	730.5989	−3.59	$[M+H]^+$	$C_{41}H_{83}N_2O_6P$	SM (d18:0/18:1 (9Z))	↓##	↑**	−	Sphingolipid metabolism
8	HMDB0003447	19.91	161.0841	1.94	$[M+Na]^+$	$C_{10}H_{11}NO$	Trp	↓##	↑**	↑*	Phe, Tyr, and Trp biosynthesis
9	HMDB0004975	19.93	809.6745	−1.30	$[M+H]^+$	$C_{48}H_{91}NO_8$	GlcCer (d18:1/24:1 (15Z))	↓#	↑**	↑**	Sphingolipid metabolism
10	HMDB0000943	0.70	136.0372	4.37	$[M-H]^-$	$C_4H_8O_5$	Threonic acid	↓##	↑**	↑**	Ascorbate and aldarate metabolism
11	HMDB0010167	7.14	835.5363	−0.47	$[M-H]^-$	$C_{46}H_{78}NO_{10}P$	PS (18:0/22:6 (4Z,7Z,10Z,13Z,16Z,19Z))	↓##	↑**	↑**	Glycerophospholipid metabolism
12	HMDB0001045	10.61	555.2693	0.27	$[M-H]^-$	$C_{28}H_{37}N_5O_7$	Enkephalin L	↑##	−	↓**	Synaptic vesicle cycle
13	HMDB0006888	11.67	532.3070	4.37	$[2M-H]^-$	$C_{27}H_{48}O_8S$	5β-cyprinol sulfate	↓##	↑**	↑**	Primary bile acid biosynthesis
14	HMDB0007938	18.06	745.5622	−0.94	$[M-H]^-$	$C_{41}H_{80}NO_8P$	PC (15:0/18:1 (11Z))	↑##	−	↓**	Glycerophospholipid metabolism
15	HMDB0009042	19.83	793.5622	−1.26	$[M+HCOO]^-$	$C_{45}H_{80}NO_8P$	PE (18:1 (11Z)/22:4 (7Z,10Z,13Z,16Z))	↑##	↓**	↓**	Glycerophospholipid metabolism
16	HMDB0000296	0.69	244.2014	−3.82	$[M+H]^+$	$C_9H_{12}N_2O_6$	Uridine	↓##	−	↑**	Pyrimidine metabolism
17	HMDB0000064	0.71	131.1332	−4.70	$[M+H]^+$	$C_4H_9N_3O_2$	Creatine	↓##	−	↑**	Glycine, serine, and threonine metabolism
18	HMDB0000089	0.86	243.2166	2.71	$[M+Na]^+$	$C_9H_{13}N_3O_5$	Cytidine	↓##	↑**	↑**	Pyrimidine metabolism
19	HMDB0008323	5.86	898.3261	−4.23	$[M+H]^+$	$C_{52}H_{100}NO_8P$	PC (20:1 (11Z)/24:1 (15Z))	↑##	↓**	↓**	Glycerophospholipid metabolism
20	HMDB0001547	7.02	346.2144	0.56	$[M+H]^+$	$C_{21}H_{30}O_4$	Corticosterone	↑##	↓**	↓**	Steroid hormone biosynthesis
21	HMDB0000086	11.72	257.2230	3.73	$[M+H]^+$	$C_8H_{20}NO_6P$	Glycerophosphocholine	↓##	↑**	↑**	Glycerophospholipid metabolism
22	HMDB0010408	11.48	505.6691	1.28	$[M+H]^+$	$C_{26}H_{52}NO_6P$	LysoPC (P-18:1 (9Z))	↑##	↓**	↓**	Glycerophospholipid metabolism
23	HMDB0010399	18.07	577.7737	1.96	$[M+H]^+$	$C_{30}H_{60}NO_7P$	LysoPC (22:1 (13Z))	↑##	↓**	↓**	Glycerophospholipid metabolism
24	HMDB0000158	0.69	181.1885	−1.63	$[M-H]^-$	$C_9H_{11}NO_3$	Tyr	↓##	↑**	−	Phe, Tyr, and Trp biosynthesis
25	HMDB0001396	4.26	459.4558	3.88	$[2M-H]^-$	$C_{20}H_{25}N_7O_6$	5-methyltetrahydrofolic acid	↓##	↑*	↑*	Glycerophospholipid metabolism
26	HMDB0000821	4.33	193.1992	−3.59	$[M-H]^-$	$C_{10}H_{11}NO_3$	Phenylacetylglycine	↑##	↓**	↓**	Phe metabolism
27	HMDB0009144	12.34	786.0288	−0.90	$[M+HCOO]^-$	$C_{45}H_{72}NO_8P$	PE (18:3 (6Z,9Z,12Z)/22:6 (4Z,7Z,10Z,13Z,16Z,19Z))	↑##	↓**	−	Glycerophospholipid metabolism
28	HMDB0009815	18.74	886.5571	4.37	$[M-H]^-$	$C_{47}H_{83}O_{13}P$	PI (18:0/20:4 (5Z,8Z,11Z,14Z))	↑##	↓**	↓**	Glycerophospholipid metabolism

Change trend compared with the control group: ↑ and ↓ represent the corresponding compound is up-regulated and down-regulated in groups, respectively. $^*P < 0.05$, $^{**}P < 0.01$, compared with the model control group (M-Con); $^{\#}P < 0.05$, $^{\#\#}P < 0.01$, compared with the normal control group (N-Con). t_R: retention time; M-Thea: model administration group; M-Flu: positive administration group; Gln: glutamine; Glu: glutamic acid; Tyr: tyrosine; Phe: phenylalanine; Trp: tryptophan; PC: phosphatidylcholine; PE: phosphatidylethanolamine; PS: phosphatidylserine; SM: sphingomyelin; PI: phosphatidylinositol; LysoPC: lysophosphatidylcholine; GlcCer: glycosphingolipid.

regulated. To further understand the metabolic differences between N-Con and M-Con, the data on the identified metabolites were analyzed, and the volcano maps are shown in Figs. 7A and B. After ʟ-theanine intervened in N-Thea, the potential biomarkers demonstrated different degrees of improvement as shown in Fig. S7. To illustrate the changing trends of the metabolites and the callback effect of ʟ-theanine, heatmap analysis was conducted as shown in Figs. 7C and D. The results showed various groups in five clusters, which were the same as the score plots of PLS-DA.

3.7. Targeted metabolomics

The untargeted metabolomics results were validated using the HILIC-QQQ-MS/MS method to determine amino acids and neurotransmitters in related pathways, including Phe, Tyr, and Trp biosynthesis pathways and Gln and Glu metabolic pathways. The measured amino acids include ʟ-Phe, ʟ-Tyr, ʟ-Trp, ʟ-Glu and ʟ-Gln, catecholamine neurotransmitters include DA, NE, and MHPG, and indoleamine neurotransmitters include 5-HT and 5-HTP, as shown in Fig. 8. Compared with N-Con, the levels of 5-HT, DA, and NE in the rats induced by CUMS were significantly reduced, similar to the autopsy results of patients with depression [37–40]. In the pathological condition of neurological diseases, circulating levels

of neuroactive compounds may be deregulated [41], suggesting that peripheral neurochemical changes may be involved in the pathological processes directly or indirectly, and the measurement of peripheral neurotransmitter levels is crucial as central neurotransmitter levels. Compared with N-Con, the levels of ʟ-Phe, ʟ-Tyr, ʟ-Trp, 5-HT, and 5-HTP in the serum of rats in M-Con were significantly reduced, whereas ʟ-Gln and ʟ-Glu were considerably increased. The changes of the analytes in the hippocampus were the same as those in the serum, except that 5-HTP was not detected in the hippocampus, ʟ-Trp were increased in rats of N-Thea, and the content of DA was significantly decreased in CUMS-induced rats. After ʟ-theanine intervention, the analytes in the three pathways were corrected, and the effect was similar to that of fluoxetine hydrochloride. This proved that ʟ-theanine had the effect of preventing depression. In addition to the increase of ʟ-Trp content in the hippocampus, the levels of analytes showed no significant difference between N-Thea and N-Con, which proved that ʟ-theanine had no significant effect on healthy rats.

3.8. Biological interpretation of biomarkers

The results of correlation analysis amongst representative biomarkers and biochemical indicators are shown in Fig. 9. Spearman's
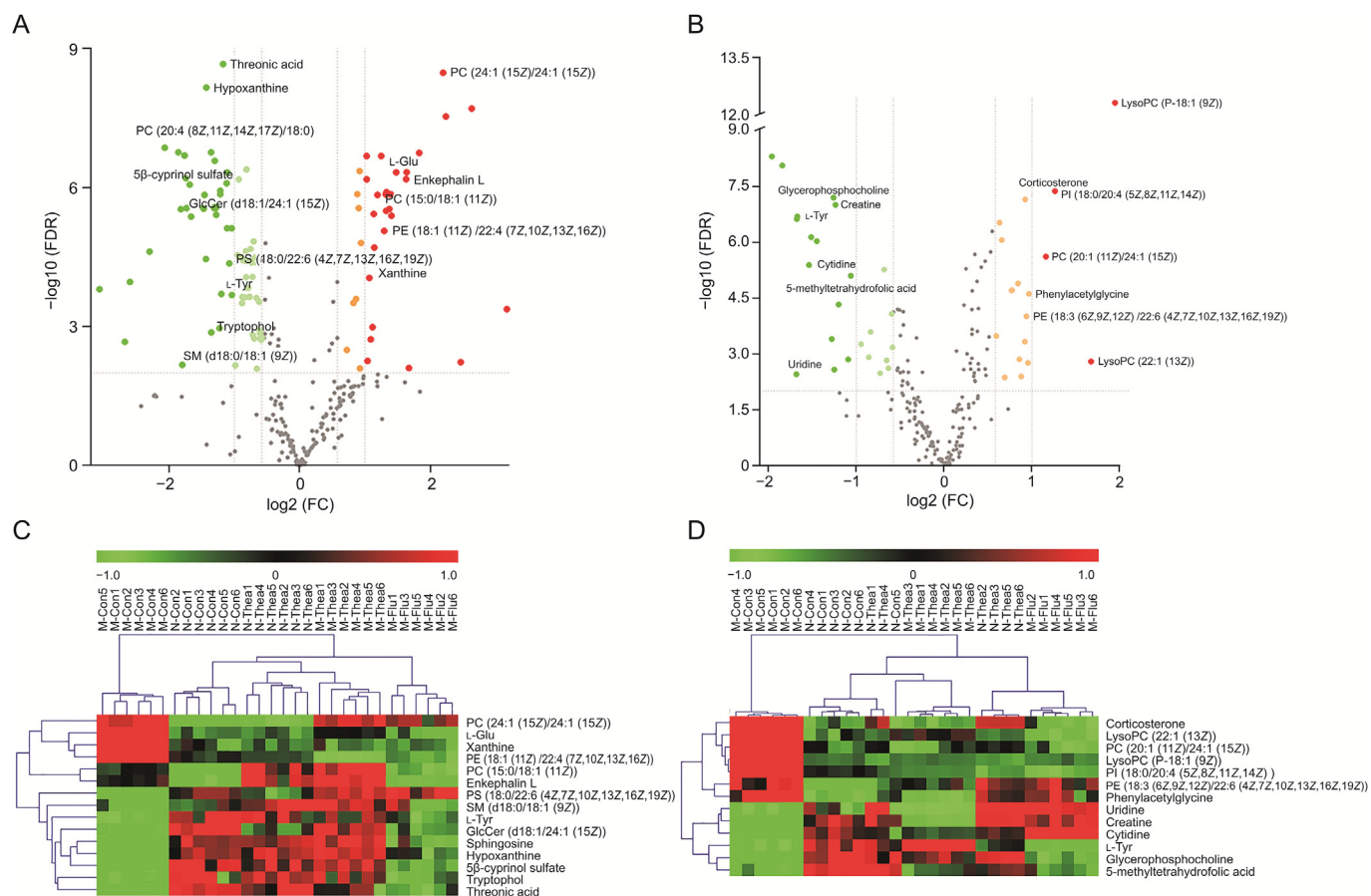
Fig. 7. The metabolic differences between the normal control group (N-Con) and model control group (M-Con). Volcano map of differential metabolites in (A) hippocampus and (B) serum. Heatmap of differentially expressed metabolites in the (C) hippocampus and (D) serum. Rows correspond to the samples, and columns correspond to the metabolites (red: up-regulated; green: down-regulated). FDR: false discovery rate; FC: fold change; PC: phosphatidylcholine; L-Glu: L-glutamic acid; GlcCer: glycosphingolipid; PE: phosphatidyl-ethanolamine; PS: phosphatidylserine; L-Tyr: L-tyrosine; SM: sphingomyelin; N-Thea: normal administration group; M-Thea: model administration group; M-Flu: positive administration group; LysoPC: lysophosphatidylcholine; PI: phosphatidylinositol.

correlation analysis showed that the level of biochemical indicators was significantly correlated with potential biomarkers, and pro-inflammatory cytokines TNF-α and IL-1β were significantly positively associated with lipid metabolism. The enrichment analysis of differential metabolites could identify biological regulatory pathways for significant differences. Thus, the level of metabolite enrichment in each pathway was calculated to determine whether the metabolic pathways were significantly affected. The metabolic pathway analysis was conducted to understand the underlying molecular functions of the biomarkers shown in Table 5 and Figs. 10, 11 and S8 mainly involving seven metabolic pathways, including Phe, Tyr, and Trp biosynthesis; Tyr metabolism; Gln and Glu metabolism; glycerophospholipid metabolism; sphingolipid metabolism; alanine, aspartate, and Glu metabolism; and arginine biosynthesis. Five were amino acid metabolism pathways and two were lipid metabolism pathways.

Nagasawa et al. [42] found that amino acid abnormalities were significantly associated with depression. Yang et al. [43] found that amino acid levels in depressed rats are changed significantly, and glycine and Gln may be potential therapeutic targets for depression. Woo et al. [44] measured 40 amino acids and found alterations of amino acids in various pathways in patients with major depressive disorder (MDD) compared with healthy individuals. In this study, the metabolites involved in amino acid metabolism were Glu, Tyr, Trp, and phenylacetylglycine. Tyr is involved in the

biosynthesis of betaine, which can convert homocysteine to methionine through betaine-homocysteine methyltransferase, and methionine can react with adenosine triphosphate to generate S-adenosylmethionine, the only methyl donor in the central nervous system, to promote the metabolism of neurotransmitters [45]. The synthesis of 5-HT depends on the content of Trp in the brain, because of 5-HTP produced from Trp via Trp hydroxylase [46]. The metabolomics results showed that the content of Tyr and Trp in the model group was significantly reduced. Because of the reduction of methyl donor, DA, NE, 5-HT, and its metabolites were reduced considerably to produce depressive symptoms, which was consistent with the content of the monoamine hypothesis. Glu is the most abundant fast excitatory neurotransmitter in the mammalian nervous system. It is released from neurons and taken up by astrocytes in the brain, forming a necessary and efficient Glu-Gln metabolic cycle [47]. Studies have shown that Glu-Glu disorder is closely related to the pathogenesis of depression. The level of Glu in the model group is significantly increased, which can produce neurotoxicity and cause nerve damage, and may be related to the deterioration of astrocytes in the animal brain caused by chronic stress stimulation [48]. The levels of amino acids in M-Thea were returned to normal levels, suggesting that L-the-anine could relieve depression symptoms by regulating amino acid metabolic pathways such as Phe, Tyr, and Trp biosynthesis and Gln and Glu metabolism. In addition, targeted metabolomics studies
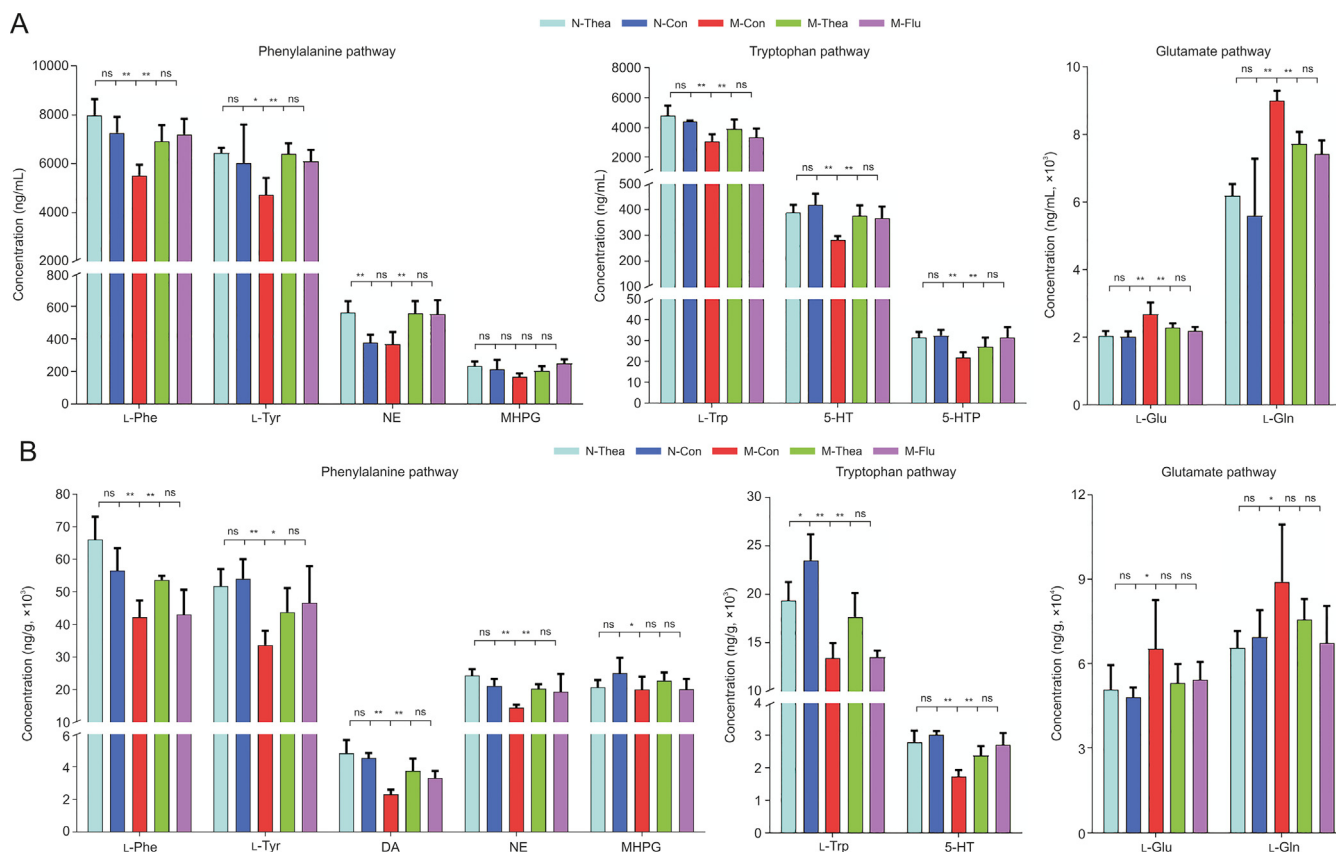
Fig. 8. The content of various amino acids and neurotransmitters in (A) serum and (B) hippocampus among all groups. Values were calculated as mean ± standard deviation ($n = 6$). $^{**}P < 0.01$, very significant differences; $^{*}P < 0.05$, significant differences, ns: no significant differences. N-Con: normal control group; N-Thea: normal administration group; M-Con: model control group; M-Thea: model administration group; M-Flu: positive administration group; L-Phe: L-phenylalanine; L-Tyr: L-tyrosine; NE: norepinephrine; MHPG: 3-methoxy-4-hydroxyphenylglycol; L-Trp: L-tryptophan; 5-HT: serotonin; 5-HTP: 5-hydroxytryptophan; L-Glu: L-glutamic acid; L-Gln: L-glutamine; DA: dopamine.

found that L-theanine can significantly improve the content of neurotransmitters, the important biochemical molecules controlling the physiological functions of the central and peripheral nervous systems. Among them, monoamine neurotransmitters are closely related to the development of neuropsychiatric diseases [49].
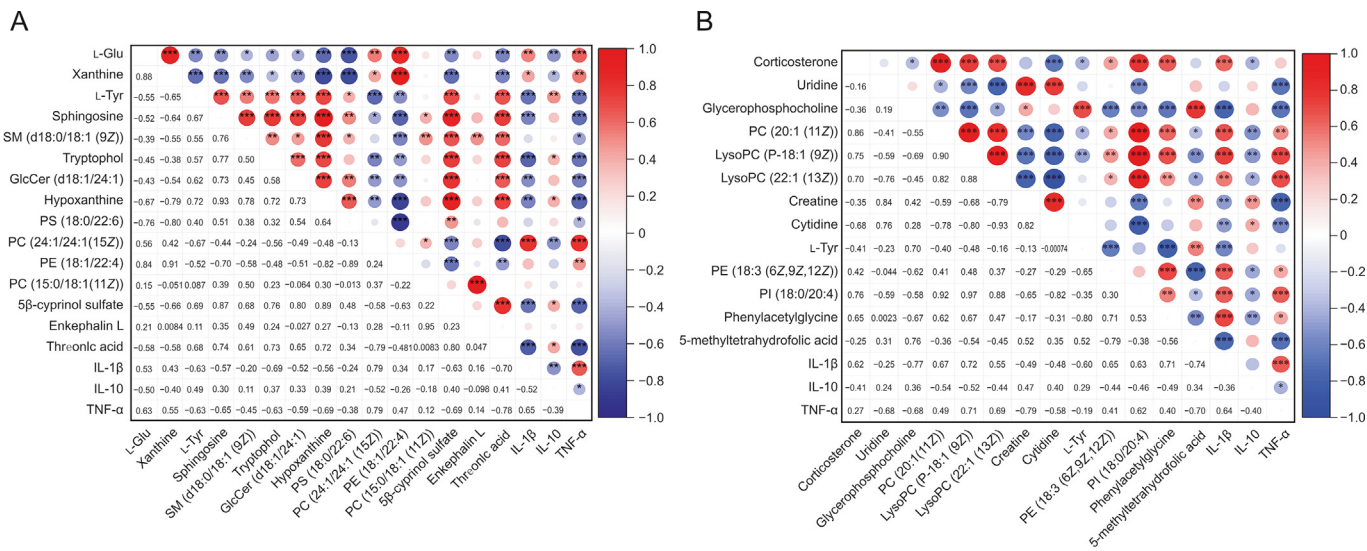

Fig. 9. Correlation analysis among representative biomarkers and biochemical indicators. (A) Hippocampus and (B) serum. The size and color of the circles represent the degree of correlation. The corresponding value was marked in the corresponding grid and $^{*}P < 0.05$, $^{**}P < 0.01$, $^{***}P < 0.001$ (red: positive; blue: negative). L-Glu: L-glutamic acid; L-Tyr: L-tyrosine; SM: sphingomyelin; L-Trp: L-tryptophan; GlcCer: glycosphingolipid; PS: phosphatidylserine; PC: phosphatidylcholine; PE: phosphatidylethanolamine; IL: interleukin; TNF-α: tumor necrosis factor alpha; LysoPC: lysophosphatidylcholine; PI: phosphatidylinositol.
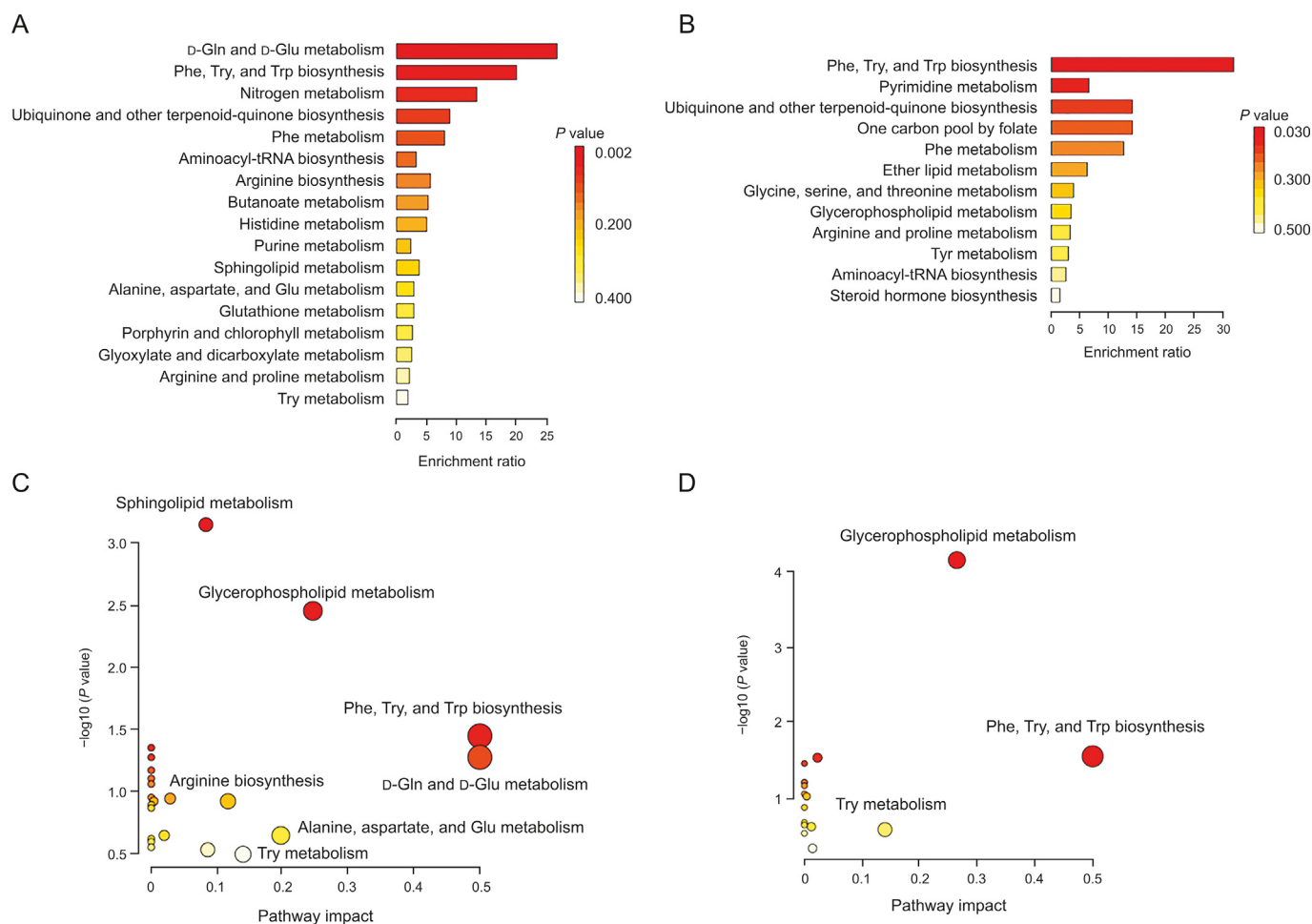
Fig. 10. Summary of enrichment analysis and pathway analysis using MetaboAnalyst 5.0. Enrichment analysis of (A) hippocampus and (B) serum and pathway analysis of (C) hippocampus and (D) serum. Gln: glutamic acid; Glu: glutamic acid; Phe: phenylalanine; Tyr: tyrosine; Trp: tryptophan; tRNA: transfer RNA.

Dyslipidaemia is a common phenomenon of depression. Given that the lipid concentration in the brain is the second highest in the body [47], lipid metabolism disorders are closely related to depression [50]. Disorders of energy metabolism are common in the pathogenesis of depression [51,52]. Phospholipids are important components of mitochondrial membranes, which are the product of phosphoethanolamine produced by the phosphorylation of ethanolamine-by-ethanolamine kinase [44]. Mitochondrial dysfunction due to disturbances in phospholipid metabolism may lead to altered energy production, which in turn triggers depression [53,54]. In this study, the content of lipid components in M-Con changed, including LysoPC, PC, SM, PE, PS, PI, and GlcCer. PC and PE are distributed asymmetrically in the plasma membrane, which are the important part of metabolism and signalling. LysoPC, produced by the hydrolysis of PC, can increase the oxidative stress of vascular endothelial cells [55]. PI can directly or indirectly participate in the signal transduction of neurotransmitters, hormones, and growth factors. PI-related dopamine receptors play an essential role in the neuronal excitatory transmission and can promote long-term depression of rat hippocampal CA1 synapses, leading to depression. A study found that glycerophospholipid was increased dramatically in patients with MDD, which was significantly positively correlated with depression severity [56]. Sphingolipids are a class of lipid compounds with signalling capabilities, whereas SMs and GlcCers are the most complex sphingolipids. Abnormal sphingolipid metabolism may lead to altered synaptic function, leading to depression [57]. Sphingolipid metabolism may be related to altered concentrations of corticosterone (CORT), a steroid hormone secreted by the adrenal cortical tract, and an important hormone for the hypothalamic–pituitary–adrenal axis. SM concentration in M-Con decreased, and the CORT concentration increased, presumably because the reduced SM content was not conducive to the recovery of white matter myelin [45], increasing the risk of depression. Depressed patients have abnormally active purine metabolism. Hypoxanthine and xanthine are the direct precursors of uric acid, in which hypoxanthine is oxidized to xanthine via xanthine oxidase, and xanthine is to uric acid. The concentration of xanthine in patients with depression increases, and uric acid production increases, leading to enhanced antioxidant effects caused by depression [58]. The levels of glycerophospholipid, sphingolipid, and purine in the administration group were adjusted to varying degrees, which proved that L-theanine could treat depression by regulating glycerophospholipid metabolism, sphingolipid metabolism, and purine metabolism pathways. At present, the study has shown L-theanine can promote fat conversion and has a certain lipid-lowering effect [59], which further showed that L-theanine could prevent depression by regulating lipid pathways.
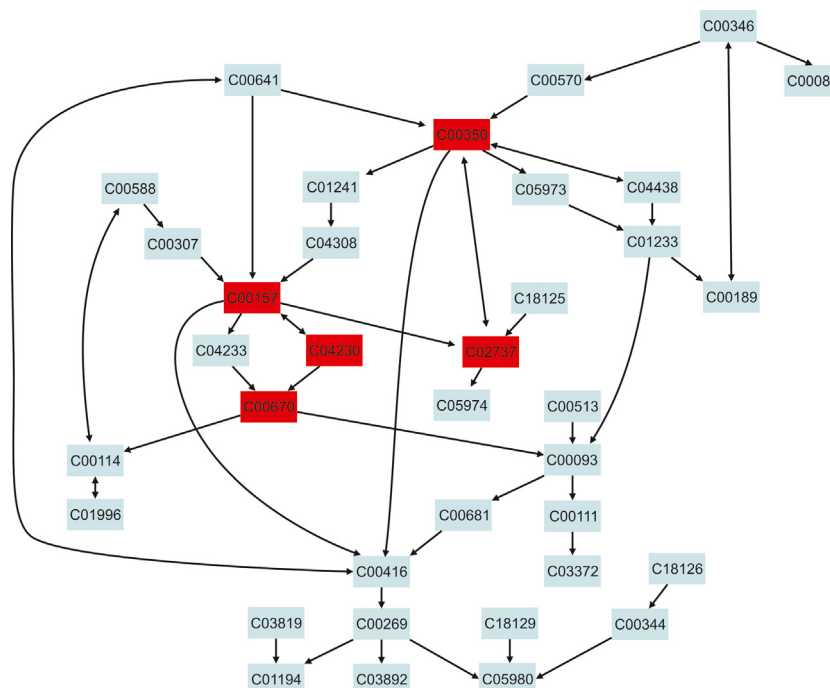
Fig. 11. The metabolites involved in glycerophospholipid metabolism pathways which are associated with the selected biomarkers identified in the analysis of rat serum and hippocampus. C00350: phosphatidylethanolamine; C00157: phosphatidylcholine; C02737: phosphatidylserine; C04230: 1-acyl-*sn*-glycero-3-phosphocholine; C00670: *sn*-glycero-3-phosphocholine (red: biomarkers identified in this pathway).

4. Conclusions

Depression is a severe psychiatric disease in children and adolescents. Therefore, it is very important to develop effective antidepressants and understand their mechanism of action during the remarkable growth stages of children and adolescents. In this study, we replicated the CUMS model of juvenile rats and used ELISA and LC-MS/MS to explore the pathogenesis of depression. The results showed that depressive state in juvenile rats was closely related to the monoamine hypothesis and the inflammatory factor hypothesis. The developed RP-UPLC-Q-TOF-MS/MS method for untargeted metabolomics screened 28 biomarkers of ʟ-theanine in the prevention of depression, mainly involving amino acid metabolism and lipid metabolism pathways. An efficient and sensitive HILIC-QQQ-MS/MS method was developed and validated for targeted metabolomics research, which showed that ʟ-theanine could safely adjust the levels of various neurotransmitters to prevent CUMS-induced depression in juvenile rats. Future research work on the mechanism of depression in children and adolescents should focus on amino acids and lipids. This study laid the foundation for the clinical research on ʟ-theanine in treating depression in children and adolescents.

CRediT author statement

Yanru Zhu: Writing - Original draft preparation, Conceptualization, Methodology; **Feng Wang**: Data curation, Software; **Jiatong Han**: Visualization, Investigation; **Yunli Zhao**: Supervision; **Miao Yu**: Validation; **Mingyan Ma**: Writing - Reviewing and Editing; **Zhiguo Yu**: Writing - Reviewing and Editing.

Declaration of competing interest

The authors declare that there are no conflicts of interest.

Appendix A. Supplementary data

Supplementary data to this article can be found online at https://doi.org/10.1016/j.jpha.2022.10.001.

References

[1] A. Werner-Seidler, S. Spanos, A.L. Calear, et al., School-based depression and anxiety prevention programs for young people: A systematic review and meta-analysis, Clin. Psychol. Rev. 89 (2017), 102079.
[2] T. Mendelson, S.D. Tandon, Prevention of depression in childhood and adolescence, Child Adolesc. Psychiatr. Clin. N. Am. 25 (2016) 201—218.
[3] L.B. Ramsey, J.R. Bishop, J.R. Strawn, Pharmacogenetics of treating pediatric anxiety and depression, Pharmacogenomics 20 (2019) 867—870.
[4] Y.-Y. Han, J.-J. Dai, Research progress in animal models and mechanism of depression, Acta Lab. Anim. Sci. Sin. 24 (2016) 321—326.
[5] C.L. Raison, L. Capuron, A.H. Miller, Cytokines sing the blues: Inflammation and the pathogenesis of depression, Trends Immunol. 27 (2006) 24—31.
[6] H. Chen, H. Xie, S. Huang, et al., Development of mass spectrometry-based relatively quantitative targeted method for amino acids and neurotransmitters: Applications in the diagnosis of major depression, J. Pharm. Biomed. 194 (2021), 113773.
[7] A. Cipriani, X. Zhou, C. del Giovane, et al., Comparative efficacy and tolerability of antidepressants for major depressive disorder in children and adolescents: A network meta-analysis, Lancet 388 (2016) 881—890.
[8] A.L. Lardner, Neurobiological effects of the green tea constituent theanine and its potential role in the treatment of psychiatric and neurodegenerative disorders, Nutr. Neurosci. 17 (2014) 145—155.
[9] S. Hidese, S. Ogawa, M. Ota, et al., Effects of ʟ-theanine administration on stress-related symptoms and cognitive functions in healthy adults: A randomized controlled trial, Nutrients 11 (2019), 2362.
[10] S. Hidese, M. Ota, C. Wakabayashi, et al., Effects of chronic ʟ-theanine administration in patients with major depressive disorder: An open-label study, Acta Neuropsychiatr. 29 (2017) 72—79.
[11] T. Takarada, N. Nakamichi, T. Kakuda, et al., Daily oral intake of theanine prevents the decline of 5-bromo-2'-deoxyuridine incorporation in hippocampal dentate gyrus with concomitant alleviation of behavioral abnormalities in adult mice with severe traumatic stress, J. Pharmacol. Sci. 127 (2015) 292—297.
[12] J.F. Borzelleca, D. Peters, W. Hall, A 13-week dietary toxicity and toxicokinetic study with ʟ-theanine in rats, Food Chem. Toxicol. 44 (2006) 1158—1166.
[13] J. Williams, J. Kellett, P. Roach, et al., ʟ-theanine as a functional food additive: Its role in disease prevention and health promotion, Beverages 2 (2016), 13.

[14] R.D. Beger, W. Dunn, M.A. Schmidt, et al., Metabolomics enables precision medicine: "A white paper, community perspective", Metabolomics 12 (2016), 149.

[15] S. Barnes, H.P. Benton, K. Casazza, et al., Training in metabolomics research. I. Designing the experiment, collecting and extracting samples and generating metabolomics data, J. Mass Spectrom. 51 (2016) 461–475.

[16] C. Johnson, G. Ivanisevic, G. Siuzdak, Metabolomics: Beyond biomarkers and towards mechanisms, Nat. Rev. Mol. Cell Biol. 17 (2016) 451–459.

[17] D.H. Hackos, P.J. Lupardus, T. Grand, et al., Positive allosteric modulators of GluN2A-containing NMDARs with distinct modes of action and impacts on circuit function, Neuron 89 (2016) 983–999.

[18] X. Liu, M. Lv, Y. Wang, et al., Deciphering the compatibility rules of traditional Chinese medicine prescriptions based on NMR metabolomics: A case study of Xiaoyaosan, J. Ethnopharmacol. 254 (2020), 112726.

[19] U.S. Food and Drug Administration, Bioanalytical Method Validation Guidance for Industry. https://www.fda.gov/regulatory-information/search-fda-guidance-documents/bioanalytical-method-validation-guidance-industry. (Accessed 24 May 2021).

[20] X. Han, Y. Qin, Y. Zhu, et al., Development of an underivatized LC-MS/MS method for quantitation of 14 neurotransmitters in rat hippocampus, plasma and urine: Application to CUMS induced depression rats, J. Pharm. Biomed. Anal. 174 (2019) 683–695.

[21] Q. Guo, X.-M. Lin, Z. Di, et al., Electroacupuncture ameliorates CUMS-induced depression-like behavior: Involvement of the glutamatergic system and apoptosis in rats, Comb. Chem. High Throughput Screen. 24 (2021) 996–1004.

[22] L. Yu, S.-C. An, T. Lian, Involvement of hippocampal NMDA receptor and neuropeptide Y in depression induced by chronic unpredictable mild stress, Sheng Li Xue Bao 62 (2010) 14–22.

[23] L. Liu, Y. Dong, X. Shan, et al., Anti-depressive effectiveness of baicalin *in vitro* and *in vivo*, Molecules (2019), 326.

[24] W. Su, Y. Zhang, Y. Chen, et al., *NLRP3* gene knockout blocks NF-κB and MAPK signaling pathway in CUMS-induced depression mouse model, Behav. Brain Res. 322 (2017) 1–8.

[25] K.A. Roth, R.J. Katz, Stress, behavioral arousal, and open field activity—A reexamination of emotionality in the rat, Neurosci. Biobehav. Rev. 3 (1979) 247–263.

[26] Q. Lu, A. Mouri, Y. Yang, et al., Chronic unpredictable mild stress-induced behavioral changes are coupled with dopaminergic hyperfunction and serotonergic hypofunction in mouse models of depression, Behav. Brain Res. 372 (2019), 112053.

[27] M. Bourin, M. Hascoët, The mouse light/dark box test, Eur. J. Pharmacol. 463 (2003) 55–65.

[28] H.E. Scharfman, The enigmatic mossy cell of the dentate gyrus, Nat. Rev. Neurosci. 17 (2016) 562–575.

[29] K. Mizuseki, S. Royer, K. Diba, et al., Activity dynamics and behavioral correlates of CA3 and CA1 hippocampal pyramidal neurons, Hippocampus 22 (2012) 1659–1680.

[30] Y. Lu, C.S. Ho, X. Liu, et al., Chronic administration of fluoxetine and pro-inflammatory cytokine change in a rat model of depression, PLoS One 12 (2017), e0186700.

[31] J. Tang, W. Yu, S. Chen, et al., Microglia polarization and endoplasmic reticulum stress in chronic social defeat stress induced depression mouse, Neurochem. Res. 43 (2018) 985–994.

[32] X. Zheng, A. Kang, C. Dai, et al., Quantitative analysis of neurochemical panel in rat brain and plasma by liquid chromatography-tandem mass spectrometry, Anal. Chem. 84 (2012) 10044–10051.

[33] I. Fuertes, C. Barata, Characterization of neurotransmitters and related metabolites in Daphnia magna juveniles deficient in serotonin and exposed to neuroactive chemicals that affect its behavior: A targeted LC-MS/MS method, Chemosphere 263 (2021), 127814.

[34] A. Wakamatsu, S. Ochiai, E. Suzuki, et al., Proposed selection strategy of surrogate matrix to quantify endogenous substances by Japan Bioanalysis Forum DG2015-15, Bioanalysis 10 (2018) 1349–1360.

[35] J. Marcos, N. Renau, O. Valverde, et al., Targeting tryptophan and tyrosine metabolism by liquid chromatography tandem mass spectrometry, J. Chromatogr. A 1434 (2016) 91–101.

[36] Z. Yuan, J. Li, X. Zhou, et al., HS-GC-IMS-Based metabonomics study of Baihe Jizihuang Tang in a rat model of chronic unpredictable mild stress, J. Chromatogr. B 1148 (2020), 122143.

[37] L. Ding, X. Zhang, H. Guo, et al., The functional study of a Chinese herbal compounded antidepressant medicine – Jie Yu Chu Fan capsule on chronic unpredictable mild stress mouse model, PLoS One 10 (2015), e0133405.

[38] W. Song, Y. Guo, S. Jiang, et al., Antidepressant effects of the ginsenoside metabolite compound K, assessed by behavioral despair test and chronic unpredictable mild stress model, Neurochem. Res. 43 (2018) 1371–1382.

[39] P. Rosa-Neto, M. Diksic, H. Okazawa, et al., Measurement of brain regional alpha-[11C]methyl-L-tryptophan trapping as a measure of serotonin synthesis in medication-free patients with major depression, Arch. Gen. Psychiatry 61 (2004) 556–563.

[40] J.H. Meyer, H.E. McNeely, S. Sagrati, et al., Elevated putamen D(2) receptor binding potential in major depression with motor retardation: An [11C] raclopride positron emission tomography study, Am. J. Psychiatry 163 (2006) 1594–1602.

[41] H. Cai, R. Zhu, H. Li, Determination of dansylated monoamine and amino acid neurotransmitters and their metabolites in human plasma by liquid chromatography-electrospray ionization tandem mass spectrometry, Anal. Biochem. 396 (2010) 103–111.

[42] M. Nagasawa, Y. Ogino, K. Kurata, et al., Hypothesis with abnormal amino acid metabolism in depression and stress vulnerability in Wistar Kyoto rats, Amino Acids 43 (2012) 2101–2111.

[43] X. Yang, G. Wang, X. Gong, et al., Effects of chronic stress on intestinal amino acid pathways, Physiol. Behav. 204 (2019) 199–209.

[44] H.-I. Woo, M.-R. Chun, J.-S. Yang, et al., Plasma amino acid profiling in major depressive disorder treated with selective serotonin reuptake inhibitors, CNS Neurosci. Ther. 21 (2015) 417–424.

[45] Y. Zhu, S. Li, C. Zhu, et al., Metabolomics analysis of the antidepressant prescription danzhi xiaoyao powder in a rat model of chronic unpredictable mild stress (CUMS), J. Ethnopharmacol. 260 (2020), 112832.

[46] X.-X. Gao, J. Cui, X.-Y. Zheng, et al., An investigation of the antidepressant action of xiaoyaosan in rats using ultra performance liquid chromatography-mass spectrometry combined with metabonomics, Phytother Res. 27 (2013) 1074–1085.

[47] C. Chai, B. Jin, Y. Yan, et al., Anti-depressant effect of Zhi-zi-chi decoction on CUMS mice and elucidation of its signaling pathway, J. Ethnopharmacol. 266 (2021), 113283.

[48] Z. Liu, N. Zhou, T. Liu, et al., Progress in depression based on metabolomics, Chin. J. Pathophysiol. 36 (2020) 2264–2275.

[49] H.-M. Jia, M. Yu, L.-Y. Ma, et al., Chaihu-Shu-Gan-San regulates phospholipids and bile acid metabolism against hepatic injury induced by chronic unpredictable stress in rat, J. Chromatogr. B 1064 (2017) 14–21.

[50] X. Li, X. Qin, J. Tian, et al., Integrated network pharmacology and metabolomics to dissect the combination mechanisms of Bupleurum chinense DC-Paeonia lactiflora Pall herb pair for treating depression, J. Ethnopharmacol. 264 (2021), 113281.

[51] D. Kolar, L. Kleteckova, H. Brozka, et al., Mini-review: Brain energy metabolism and its role in animal models of depression, bipolar disorder, schizophrenia and autism, Neurosci. Lett. 760 (2021), 136003.

[52] W. Ma, J. Song, H. Wang, et al., Chronic paradoxical sleep deprivation-induced depression-like behavior, energy metabolism and microbial changes in rats, Life Sci. 225 (2019) 88–97.

[53] C. Chiarla, I. Giovannini, J.H. Siegel, Characterization of alpha-amino-*n*-butyric acid correlations in sepsis, Transl. Res. 158 (2011) 328–333.

[54] J. Modica-Napolitano, P. Renshaw, Ethanolamine and phosphoethanolamine inhibit mitochondrial function *in vitro*: Implications for mitochondrial dysfunction hypothesis in depression and bipolar disorder, Biol. Psychiatry 55 (2004) 273–277.

[55] T.M. Michel, D. Pülschen, J. Thome, The role of oxidative stress in depressive disorders, Curr. Pharm. Des. 18 (2012) 5890–5899.

[56] X. Huang, W. Li, B. You, et al., Serum metabonomic dtudy on the antidepressant-like effects of ellagic acid in a chronic unpredictable mild stress-Induced mouse model, J. Agric. Food Chem. 68 (2020) 9546–9556.

[57] C.P. Müller, C. Reichel, C. Mühle, et al., Brain membrane lipids in major depression and anxiety disorders, Biochim. Biophys. Acta 1851 (2015) 1052–1065.

[58] T. Ali-Sisto, T. Tolmunen, E. Toffol, et al., Purine metabolism is dysregulated in patients with major depressive disorder, Psychoneuroendocrinology 70 (2016) 25–32.

[59] W.-Q. Peng, G. Xiao, B.-Y. Li, et al., L-theanine activates the browning of white adipose tissue through the AMPK/α-Ketoglutarate/Prdm16 axis and ameliorates diet-induced obesity in mice, Diabetes 70 (2021) 1458–1472.